Eur. Phys. J. A **25**, s01, 241–242 (2005)
DOI: 10.1140/epjad/i2005-06-190-1

EPJ A direct
electronic only

Measurement of evaporation residue cross sections from reactions with radioactive neutron-rich beams

D. Shapira[1,a], J.F. Liang[1], C.J. Gross[1], R.L. Varner[1], J.R. Beene[1], A. Galindo-Uribarri[1], J. Gomez Del Campo[1], P.E. Mueller[1], D.W. Stracener[1], P.A. Hausladen[1], C. Harlin[2], J.J. Kolata[3], H. Amro[3], W. Loveland[4], K.L. Jones[5], J.D. Bierman[6], and A.L. Caraley[7]

[1] Physics Division, Oak Ridge National Laboratory, Oak Ridge, TN 37831, USA
[2] Department of Physics, University of Surrey, Guildford GU2 7XH, UK
[3] Physics Department University of Notre Dame, Notre Dame, IN 46556-5670, USA
[4] Chemistry Department, Oregon State University, Corvallis, OR 97331, USA
[5] Department of Physics and Astronomy, Rutgers University, Piscataway, NJ 08856, USA
[6] Physics Department AD51, Gonzaga University, Spokane, WA 99258-0051, USA
[7] Department of Physics, SUNY at Oswego, Oswego, NY 13126, USA

Received: 14 February 2005 /
Published online: 26 July 2005 –

Abstract. Evaporation residue cross sections for ^{132}Sn, ^{134}Te and ^{124}Sn with ^{64}Ni were measured. A compact system to measure these cross sections to values as low as 1 mb is described and a sample of data acquired with this system is shown.

PACS. 25.60.-t Reactions induced by unstable nuclei – 25.60.Pj Fusion reactions – 25.70.-z Low and intermediate energy heavy-ion reactions – 25.70.Jj Fusion and fusion-fission reactions

A diagram of the experimental setup used to study the evaporation residues from collisions of accelerated fission products from uranium produced at HRIBF [1] with a secondary ^{64}Ni target, is shown in fig. 1. The setup depicted allows beam rates of up to 10^5 counts/s (limited by the gas-filled ionization chamber). The efficiency for detecting evaporation residues is very high, especially under conditions where inverse kinematics are employed. The fast timing detectors allow us to apply a fast pre-trigger that selects events associated with particles slower than the beam (*e.g.* evaporation residues). These timing detectors also allow for continuous monitoring of beam intensity and the beam profile is monitored using the position signals from the third timing detector. Counting of incident beam particles and continuous monitoring of the beam position can yield accurate cross section data. A full description of this setup will appear in a forthcoming publication [2].

Figure 2 displays rescaled cross sections for ^{132}Sn and ^{124}Sn on ^{64}Ni. Part of the ^{132}Sn data shown here were measured in a separate experiment [3] with the same setup. The ^{124}Sn data were taken in a separate stable beam run, for comparison with data from ref. [4] as well as to extend these measurements to lower bombarding energy. Figure 3 contains similar data comparing evaporation residue cross sections for ^{134}Te + ^{64}Ni ($A = 134$ beam purity $\geq 95\%$) and for ^{124}Sn + ^{64}Ni. All cross section shown are plotted in a manner that removes any expected difference in cross section that are due to trivial variation in nuclear sizes and barrier heights (rescaled). The barrier height, $V_{\rm b}$, used in these figures is the calculated barrier height of the combined nuclear [5] potential and the Coulomb potential of two charged spheres. The interaction radius, R, used in these figures is the radius corresponding to the top of the calculated interaction barrier ($V_{\rm b}$). The data in fig. 2 provide evidence for a large enhancement in the evaporation residue cross section of ^{132}Sn compared to the less neutron-rich ^{124}Sn case at energies below the Coulomb barrier. Note that for all the systems shown here fissilities are almost identical, and that fission competition is predicted by statistical model calculations to be very small at sub-barrier energies. Coupled-channel calculations which include coupling to inelastic excitation of target and projectile, two-phonon excitation, mutual excitation and transfer of up to three neutrons describe, successfully, the ^{124}Sn + ^{64}Ni fusion cross sections [6] but could not reproduce the enhancement observed in the ^{132}Sn + ^{64}Ni system [7]. The ^{134}Te data in fig. 3 show a very different behavior. No enhancement of sub-barrier evaporation residue cross sections in ^{134}Te + ^{64}Ni is observed beyond what is seen

[a] Conference presenter;
e-mail: shapira@mail.phy.ornl.gov

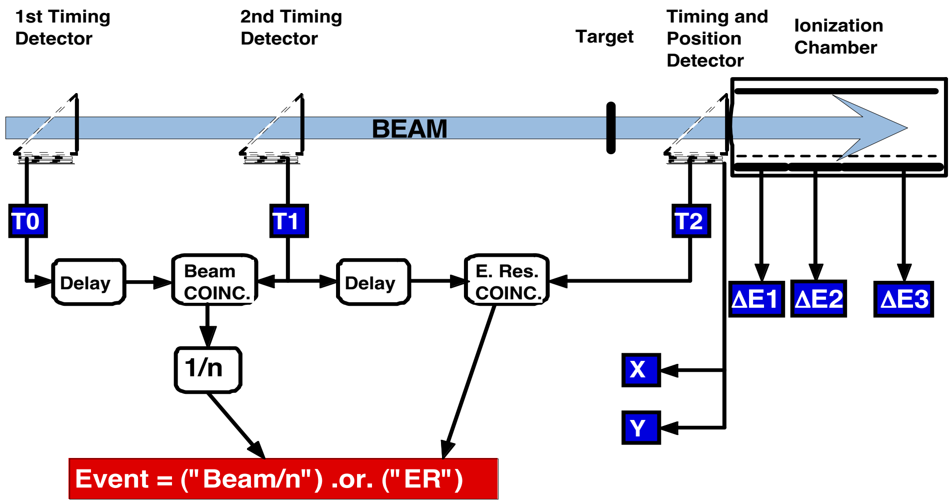

Fig. 1. A block diagram showing the main elements of our detection system. The black (blue on-line) boxes present the different signals (parameters) that are recorded every time a valid event occurred. A valid event could be either a particle slower than the beam or a down scaled sample of the beam.

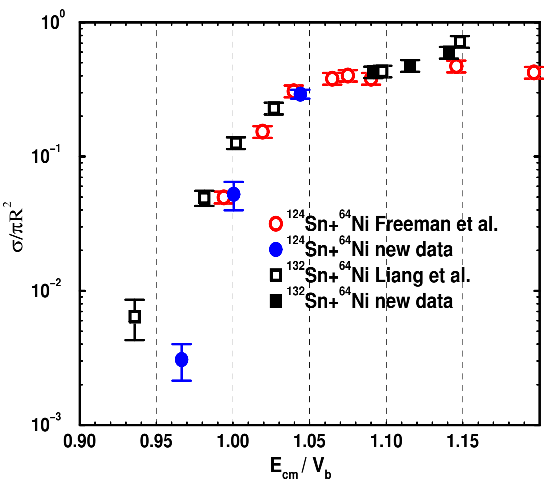

Fig. 2. Rescaled evaporation residue cross sections. The data set labeled Freeman *et al.* is from [4]. All other data were taken with this system.

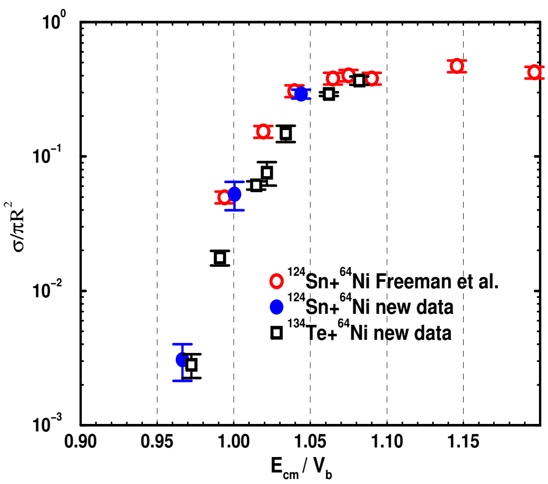

Fig. 3. Rescaled evaporation residue cross sections. The ^{124}Sn data are the same as in fig. 2.

in ^{124}Sn + ^{64}Ni. One could only speculate at this point whether the paucity of neutron transfer channels with positive Q-value is at play, or maybe fission is more important in ^{134}Te + ^{64}Ni after all.

This work is supported by DOE contract DE-AC05-00OR22725 with UT-Battelle. H.A. and J.J.K. are supported by NSF grant PHY02-44989. W.L. is supported by the USDOE grant No. DE-FG06-97ER41026.

References

1. D. Stracener, Nucl. Instrum. Methods B **204**, 42 (2003).
2. D. Shapira *et al.*, *A high efficiency compact setup to study evaporation residues formed in reactions induced by low intensity radioactive ion beams*, to be published in Nucl. Instrum. Methods A.
3. J.F. Liang *et al.*, Phys. Rev. Lett. **91**, 152701 (2003).
4. W.S. Freeman *et al.*, Phys. Rev. Lett. **50**, 1563 (1983).
5. R. Bass, Phys. Rev. Lett. **39**, 265 (1977).
6. H. Esbensen *et al.*, Phys. Rev. C **57**, 2401 (1998).
7. J.F. Liang *et al.*, Prog. Theor. Phys., Suppl. No. **154**, 106 (2004).